neuroreport

WE report that the response of neurons in rat somatosensory cortex to tactile stimulation consists of two components, a short-latency response and an oscillatory response, observable as up to 8 peaks in the post-stimulus-time-histogram with interpeak intervals in the order of 100 ms (10 Hz). While the first component is always stimulus locked, the second component is strictly stimulus-locked only when elicited from the resting state: once started, the oscillations are only weakly affected by further stimulation. This implies generally that the question of stimulus locking of oscillatory response components is not a yes/no question. Instead, the concept of dynamic coupling is shown to adequately capture the different limit cases. We present a simple dynamic model that exemplifies this point.

Key words: Cortex; Dynamics; Oscillations; Thalamus

Evoked oscillatory cortical responses are dynamically coupled to peripheral stimuli

Gregor Schöner,[CA] Klaus Kopecz, Friederike Spengler and Hubert R. Dinse

Institut für Neuroinformatik, Ruhr-Universität Bochum, Germany

[CA] Corresponding Author

Introduction

Slow (10 Hz) evoked oscillatory cortical and thalamic response components have been intensely studied for a long time,[1-6] but the functional meaning of these oscillations has remained largely unclear. The work reported here was motivated by attempts to develop mathematical models for temporally structured neural response on a functional level. We found that the very nature of the coupling of oscillatory response to peripheral stimuli needed much clarification before being accessible to formal description.

Materials and Methods

For electrophysiological recording rats were anaesthetized (with Nembutal in 2 rats, with Urethan in 31 rats) and placed in a stereotactic apparatus. The skull was opened over one hemisphere over the SI area, the dura removed and the cortical surface covered with paraffin-oil. Recordings were made with glass microelectrodes (1–2 MΩ) filled with concentrated NaCl. Both single-unit and multi-unit activity was stored on a PC. Local field potentials (LFP) were obtained simultaneously, by filtering the potential from the same electrode with a cutoff frequency of 100 Hz. LFPs were digitized at 1 kHz and also stored on a PC. We recorded from 33 rats within the hindpaw representation. During measurement receptive fields were stimulated by taps of 8 ms duration. To probe how the response time structure depends on the oscillatory state of a cell a second stimulus (test stimulus) was applied during the ongoing response elicited by a conditioning stimulus. In different trials of 32 repetitions each we varied the interstimulus interval (ISI) between conditioning and test stimulus in steps from 40 ms to 1000 ms (step-size 10 ms from 40 to 350 ms, larger for larger ISI). The overall repetition interval was kept fixed at 2 s.

The temporal structure of cortical response in the post-stimulus-time histogram (PSTH) (Fig. 1) was analysed by determining peak times, peak amplitudes and peak masses (total number of spikes within a peak) separately for the response to the conditioning stimu-
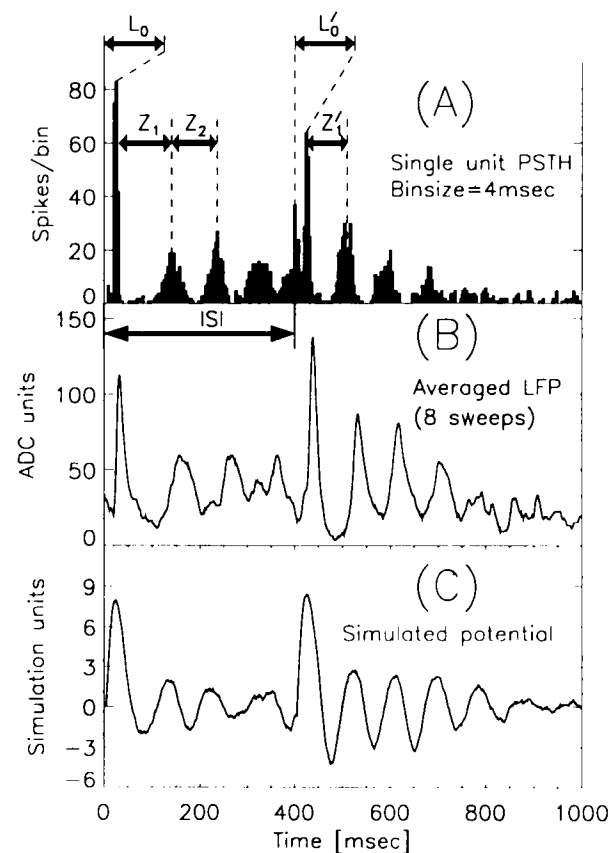

FIG. 1. (A) A single-unit PSTH from 32 repetitions accumulated with respect to the conditioning stimulus at an ISI of 400 ms. (B) The local field potential averaged over eight sweeps from the same stimulation series. (C) Result of a simulation of the dynamic model in the same stimulation paradigm as for the experimental data. In the experimental results note the clear-cut oscillatory time structure both in response to the conditioning stimulus and to the test stimulus. We found no hints at the existence of two oscillations following the test stimulus: neither suppression nor enhancement was observed as ISI was varied.

lus [unprimed measures: L_0 for latency, Z_i for cycle times ($i = 1, 2...$), M_i for masses and A_i for amplitudes ($i = 0, 1,...$)] and for the response to the test stimulus (primed measures). Statistical analysis of these measures was possible through an ensemble technique in which data on peak measures for the response to the conditioning stimulus were pooled across ISI. Because these peaks have an equivalent history with at least 1000 ms pause since the last stimulus, the corresponding statistical measures are representative of the *oscillations per se* (OPS). Out of a total of 48 cells, 24 were selected for detailed quantitative analysis on the basis of the completeness of the ISI scan. The temporal aspects of the analysis were repeated on the basis of averaged LFPs which led to equivalent results.

Results

We observed vigorous oscillatory responses in the form of sequences of 4 to 9 peaks in the PSTH in 46% of cells. The mean latency of the first peak was 21.7 ms ($\pm$ 0.8 in repetitions of PSTH for same cell, $\pm$ 2.1 across cells). The mean cycle times (cf. Fig. 1) were $Z_1 = 119.9$ ($\pm$ 5.4/17.6) ms; $Z_2 = 96.6$ ($\pm$ 7.2/12.0) ms; $Z_3 = 84.4$ ($\pm$ 11.2/11.4) ms. In general the amplitude of the oscillations does not decay monotonically and may remain constant or even increase for variable amount of time. The quantitative analysis revealed that two response components must be distinguished: the early response (first peak, in the following called the *latency peak*) and the late response (second and subsequent peaks, in the following called *oscillatory peaks*): (a) While the latency peak is elicited reliably following each single tap, the oscillatory peaks are observed only probabilistically even in oscillatory cells (on average, 62% of repetitions of complete PSTH show a 4th peak, in the same repetitions 66% show a 4th peak in the averaged LFP); (b) The latency peak differs significantly from the oscillatory peaks in mass ($M_0 > M_1 \approx M_2 \approx M_3$), amplitude ($A_0 > A_1 \approx A_2 \approx A_3$), peak shape ($A_0/M_0 \approx 5A_1/M_1$), and timing. (c) These differences extend to the variabilities with the latency peak being much less variable in timing (e.g. s.d. of peak time 2.1 ms for latency peak vs. 18.5 ms for the first oscillatory peak) in mass, and in amplitude. (d) Mass correlates strongly among oscillatory peaks but not across oscillatory and latency peaks (same for amplitude).

More interestingly, the two components also differ in the nature of their stimulus locking (Fig. 2): The latency peak is strictly stimulus locked in the sense that it appears as a sharp peak in the PSTH and its latency, following the test stimulus, depends only weakly on ISI. By contrast, the oscillatory peaks are strictly stimulus-locked only when elicited from rest: they are observable in PSTHs accumulated with reference to the conditioning stimulus, but their timing depends strongly on ISI. Essentially, the oscillatory peaks tend

to lie close to those points in time at which oscillatory peaks from the response to the conditioning stimulus are expected. The two facts may be summarized by saying that only one oscillatory component is present at any time and this oscillatory component 'goes through' the test stimulus affected only partially (by phase pulling) in its timing.

Finally, the point in time, T_{last}, when the oscillation eventually disappears as measured from the start of the conditioning stimulus (cf. (B) in Fig. 2) is neither inde-
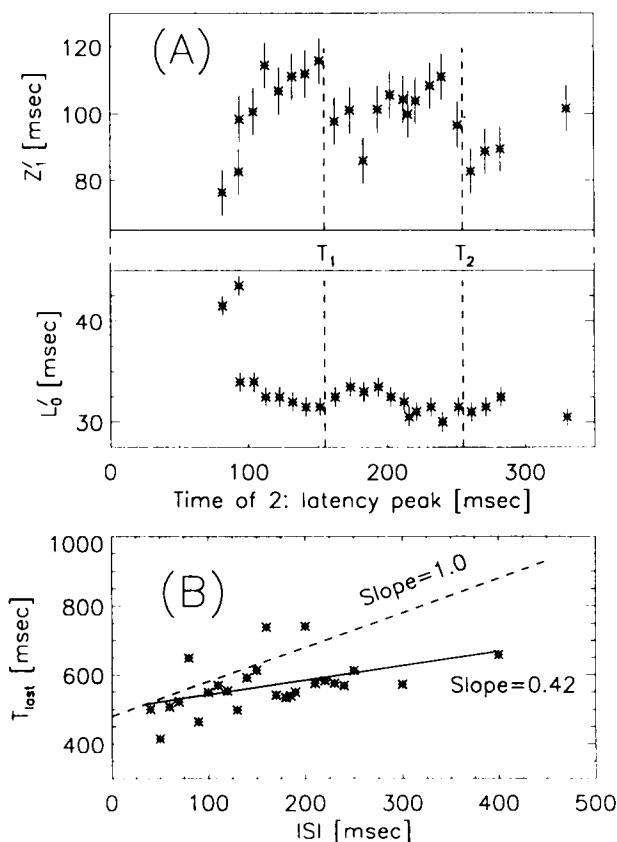

FIG. 2. Typical dependence on ISI of oscillatory time structure in responses to test stimuli, shown here for one cell. (A) On the ordinate the first cycle time (Z_1') is shown in the top part and the latency (L_0') of the first peak in the bottom part. The error bars refer to the standard deviation of the respective measures in the OPS ensemble. The abscissa is the time, ISI + L_0', at which the latency peak occurs measured from the start of the conditioning stimulus. Only for very small ISIs, a slight increase of latency is observed. By contrast, the first cycle time varies strongly as a function of ISI (note the different scales in top and bottom part). The negative slope of this dependence as the peak timing passes through the times at which oscillatory peaks from the response to the conditioning stimulus are expected (dashed lines marked T_1 and T_2) indicates that the oscillatory peaks of the response to the test stimulus lie preferably at the same times as peaks of the oscillatory response to the conditioning stimulus. The positive slope in between indicates that the test stimulus exerts some phase attraction of the oscillation. (B) The time, T_{last}, is the time from the conditioning stimulus until the oscillations finally disappear in single tap responses. The average across repeated stimulation is plotted as a function of ISI for the same cell as in (A). If the oscillations elicited by the test stimulus were an independent, restarted oscillation, the linear increase with slope 1 indicated by the dashed line is predicted. In the hypothetical other extreme, if the oscillation were totally unaffected by the test stimulus the mean T_{last} would remain constant. The observed increase is intermediate between these limit cases. For ISIs larger than the average duration of oscillations (> approximately 500 ms, not shown) the ISI dependence does indeed follow the slope one line. For those ISIs the oscillations elicited by the conditioning stimulus have stopped before oscillations are elicited anew by the test stimulus.

pendent of ISI nor shows the linear, slope one increase with ISI that would be expected if the oscillation elicited by the test stimulus was restarted afresh by the conditioning stumulus.

Discussion

Many questions relevant to the function of thalamic and cortical oscillations remain open. What we have shown in this study is that the relationship of evoked oscillations to stimulation is a dynamic one: On the one hand, oscillation can be evoked with a stable initial phase and consequently can be observed in averaged measures such as the PSTH. On the other hand, the evoked oscillations are not strictly locked to a second test stimulus. The degree of coupling to the stimulus must therefore be dynamic, that is, a function of the oscillatory state of the system.

This can be more fully understood by formulating an explicit dynamical model. The ubiquity of evoked rhythms in different parts of the nervous system, including most thalamic nuclei and the corresponding primary cortices[3,4,5,7,8] and the cerebellum,[9,10] as well what is known about cellular components of evoked rhythms[5] suggest that multiple mechanisms and structures could lead to the same phenomenology. We therefore base our modelling on the following ideas:[11] (a) Variables are defined to characterize the observed temporal patterns, and (b) dynamic equations of these variables are modelled such as to contain the observed stable states as attractor solutions.

Two types of graded, signed variables are introduced: The transfer degrees of freedom (TDF) model the latency peak, the oscillatory degrees of freedom (ODF) model the oscillatory component. The TDF dynamics capture the simplest neuronal transfer properties (linear dynamics, coupling to physical stimulus rate of change), consistent with the absence of strong ISI effects in latency peaks. Assuming a two dimensional phase space to accommodate finite latencies we use complex notation, $u = u_1 + iu_2$, where the variables are chosen such that u_1 is observed. This variable can be compared to the experimental LFP. Stable latencies are modelled by additive coupling to the peripheral stimulus which is approximated as a δ-function. The ODF dynamics must likewise be modelled in at least two dimensions to afford oscillations, in complex notation, $z = z_1 + iz_2$, but now assuming that the ODF is observed through its coupling into the TDF. We constrain the dynamics by mapping the two observed time structures, the resting and the oscillatory state, onto a fixed point and a limit cycle attractor, respectively. The functional form of such nonlinear dynamics can be chosen minimally as the normal form of the codimension-2-bifurcation where both attractors lose stability.[12] The ODF is assumed to be coupled to the stimulus only through the TDF. The functional form of this coupling is chosen to account for the well-

defined initial phase (additive coupling) and the destablization of the fixed point (multiplicative coupling). It is this dynamic coupling function that leads to the various relationships of time structure to stimulus timing observed in experiment.

$$\dot{u} = c_u u + F \sum_i \delta(t_i) + k_u z \qquad [1]$$

$$\dot{z} = c_z z + \beta z |z|^2 - \gamma z |z|^4 + k_1 u + k_2 zu \qquad [2]$$

(t_i: times at which a stimulus is applied). To account for stochastic switching in the bistable dynamics (and for other conceptual reasons)[11] fluctuations must be included by adding gaussian white stochastic forces. The model parameters of these phenomenological dynamics are directly related to the various observables. For instance, the imaginary part of c_z is the oscillation frequency, the coupling coefficient k_1 determines the first cycle time, Z_1, etc. In reproducing the experimentally observed results we chose the model parameters based on these relationships, that is, abstained from error-minimizing fits. Fig. 3 shows that the dynamical model captures all essential features of the experimental results including the probabilistic activation and decay of oscillations, the ISI dependence of the response to the test stimulus, and the ISI-dependent lifetime of the oscillations. We note that these features emerge over a wide range of parameter settings
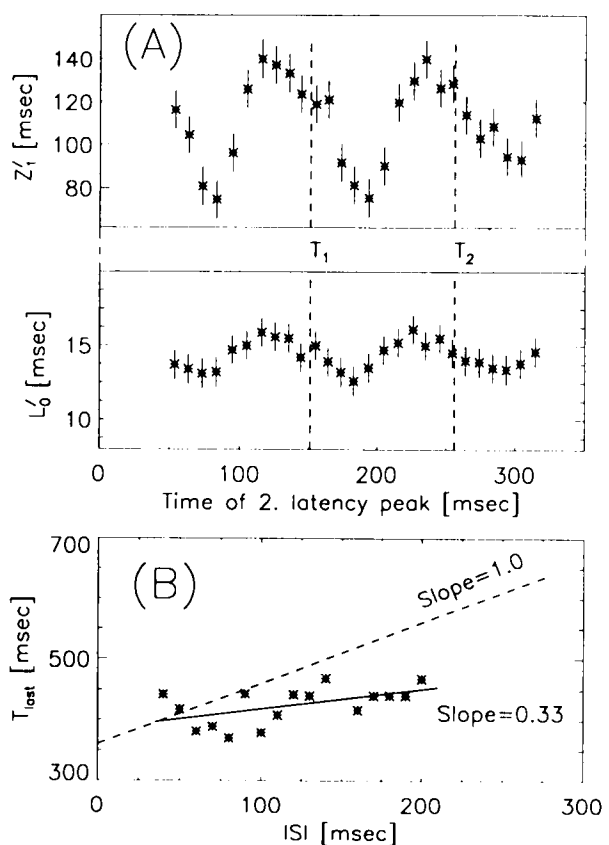
FIG. 3. Same as Fig. 2 but as obtained from simulations in the theoretical model. To reproduce the experimentally observed effects parameters were adjusted order-of-magnitude-wise on the basis of their relation to observables: $c_u = (-50 + 60i)$ Hz, $F = -25i$, $k_u = (34 + 21i)$ Hz, $c_z = (-24 + 20\pi i)$ Hz, $\beta = 10$ Hz, $\gamma = 1$ Hz, $k_1 = -5i$ Hz, $k_2 = 3$ Hz.

showing that qualitatively the effects result from the structure of the dynamical coupling rather than only as a consequence of quantitative fitting. For an illustration of an individual solution see Fig. 1, part (C), which should be compared to the corresponding LFP in part (B) of the Figure.

Conclusions

Functional interpretations of evoked temporal structure in various parts of the brain have been given in terms of amplifications,[3] gating,[9] temporal coding,[13] feature binding[14,15] and recognition.[16] A somewhat broader viewpoint, not necessarily contradictory, is that oscillations may reflect organizational principles by which continuity of sensory and motor states in time is warranted. Our results provide constraints on such functional interpretations. In particular, the results show that the concept of stimulus locked or non-stimulus locked excitation must be replaced by the broader concept of dynamic stimulus coupling.

References

1. Bishop GH, O'Leary J. *Amer J Phys* **117**, 292–308 (1936).
2. Aitkin LM, Dunlop CW, Webster WR. *J Neurophysiol* **29**, 109–123 (1966).
3. Andersen P, Andersson SA. *Physiological Basis of the Alpha Rhythm.* New York: Appleton-Century-Crofts, 1968.
4. Dinse HRO, Küger K, Best J. *Concepts in Neuroscience* **1**, 199–238 (1990).
5. Steriade M, Gloor P, Llinás RR *et al. Electroenceph Clin Neurophysiol* **76**, 481–508 (1990).
6. Connors BW, Gutnick MJ. *Trends Neurosci* **13**, 99–104 (1990).
7. Chang H-T. *J Neurophysiol*, **13**, 235–257 (1950).
8. Adrian ED. *J Physiol* **113**, 9 (1951).
9. Llinás R, Sasaki K. *Europ J Neurosci* **1**, 587–602 (1989).
10. Sasaki K, Bower JM, Llinás R. *Europ J Neurosci* **1**, 572–586 (1989).
11. Schöner G, Kelso JAS. *Science* **239**, 1513–1520 (1988).
12. Guckenheimer J, Holmes P. *Nonlinear oscillations, dynamical systems, and bifurcations of vector fields.* Springer Verlag, Berlin, 1983.
13. McClurkin JW, Optican LM, Richmond BJ *et al. Science* **253**, 675–677 (1991).
14. Eckhorn R, Bauer R, Jordan W *et al. Biol Cybern* **60**, 121–130 (1988).
15. Gray CM, König P, Engel AK *et al. Nature* **338**, 334–337 (1987).
16. Freeman WJ, Skarda CA. *Brain Res Rev* **10**, 147–175 (1985).